

1.2

QUALITY AND CONTROL OF WATER VAPOR WINDS

Gary J. Jedlovec*
 NASA/Global Hydrology and Climate Center
 Huntsville, AL 35806

Robert J. Atkinson
 Lockheed Martin Corp.
 Huntsville, AL 35812

1. STATEMENT OF THE PROBLEM

Water vapor imagery from the geostationary satellites such as GOES, Meteosat, and GMS provides synoptic views of dynamical events on a continual basis. Because the imagery represents a non-linear combination of mid- and upper-tropospheric thermodynamic parameters (three-dimensional variations in temperature and humidity), video loops of these image products provide enlightening views of regional flow fields, the movement of tropical and extratropical storm systems, the transfer of moisture between hemispheres and from the tropics to the mid-latitudes, and the dominance of high pressure systems over particular regions of the Earth. Despite the obvious larger scale features, the water vapor imagery contains significant image variability down to the single 8 km GOES pixel. These features can be quantitatively identified and tracked from one time to the next using various image processing techniques.

Merrill et al. (1991), Hayden and Schmidt (1992), and Laurent (1993) have documented the operational procedures and capabilities of NOAA and ESOC to produce cloud and water vapor winds. These techniques employ standard correlation and template matching approaches to wind tracking and use qualitative and quantitative procedures to eliminate bad wind vectors from the wind data set. Techniques have also been developed to improve the quality of the operational winds through robust editing procedures (Hayden and Veldon 1991). These quality and control approaches have limitations, are often subjective, and constrain wind variability to be consistent with model derived wind fields.

This paper describes research focused on the refinement of objective quality and control parameters

* Corresponding author address: Gary J. Jedlovec, NASA/Global Hydrology and Climate Center, 977 Explorer Blvd, Huntsville, AL 35806

for water vapor wind vector data sets. New quality and control measures are developed and employed to provide a more robust wind data set for climate analysis, data assimilation studies, as well as operational weather forecasting. The parameters are applicable to cloud-tracked winds as well with minor modifications. The improvement in winds through use of these new quality and control parameters is measured without the use of rawinsonde or modeled wind field data and compared with other approaches.

2. METHODOLOGY

2.1 The Marshall Automated Wind Technique

The standard approach taken in tracking winds with a sequence of geostationary satellite images uses a sequence of two or more images to track identifiable image features (determine image displacements). For a pair of images, the first is divided into image sub-scenes called templates, while the second image contains corresponding sub-scenes called search areas. The template is an array of picture elements and the spatial location of a template is designated as the template's center picture element location in the image. For motion calculations, the template is translated within a search area in the later image looking for the best match.

The automatic determination of local similarity between feature templates and all locations in the search area (best fit) has traditionally been done using either cross-correlation or pattern recognition methods. The Marshall Automated Wind (MAW) algorithm is differentiated from other tracking algorithms in the way it determines the best position of the template from one image to the next. Atkinson (1987) first used the sequential similarity detection algorithm (SSDA) of Barnea and Silverman (1972) in a cloud tracking algorithm. The SSDA is a different class of digital image registration and involves a simple calculation of a field of "template matching" numbers at every possible translation of the template within the search area. Each such number is the sum of the absolute value differences between every pixel in the template and the

corresponding search area in the second image. This method is unique in that it is computationally fast, requires no normalization of a correlation surface, and therefore yields an exact "0" minimum value template match in an ideal non-normalized registration case. The quantities obtained from this technique are a minimum template matching number (based on the simple difference between pixels in image 1 and image 2) and its position within the search area, which is the template displacement between image sequences. Displacement in terms of earth location and image separation times is used to determine velocity vectors (magnitude and direction of the flow field).

When using the algorithm, there are several decisions to be made that affect the motion vector results (winds): template size, search area displacement, image resolution, and temporal spacing of images. Our experience indicates that the highest quality winds come from the appropriate match of spatial and temporal resolution. For example, Wilson (1984) used 1 km GOES visible data at 5 minute intervals to determine mesoscale circulation associated with developing thunderstorms to a high degree of accuracy (standard error $< 1.0 \text{ m s}^{-1}$). Merrill (1989) also discussed the effect of image resolution on the trackability of image features. The data used in this study are from three days of GOES 8 geostationary satellite at hourly intervals and 8 km spatial resolution. Past work with GOES VAS water vapor data indicates that the appropriate template size needs to be greater than 300 km to include significant pixel variability for accurate template matching. For this study a 49 x 49 pixel template is used. Smaller templates may be appropriate for cloud tracking where thermal structure or reflectance structure is greater. The search area size (and shape) is dictated by the expected magnitude and direction of the wind. In this study, the search area is a region covered by the template when moved 30 pixels (8 km) in any direction from the initial point (center of template in the first image). This allows for winds in excess of 70 ms^{-1} .

An example of wind vectors derived using the MAW algorithm in the above way is shown in Figure 1. A sequence of 3 - hourly images of GOES 8 imager data on June 27, 1995 covering the northern hemisphere was used for tracking. Image times were 1415, 1515, and 1615 UTC. The spacing of the wind vectors is roughly 350 km over most of the Northern Hemisphere extended region. Figure 1a shows all winds derived from the tracking algorithm without quality and control measures imposed. When viewed with a loop of the

water vapor imagery (not shown), it is readily apparent that the wind vectors capture many of the main circulation features in the imagery. There are some vectors which do not show spatial consistency and will be the subject of quality and control measures presented below. This paper focuses on procedures to quasi-objectively determine good winds from bad based on statistical parameters derived in the tracking process and consistency measures between pairs of wind vectors.

2.2 Sources of error in satellite derived winds

Errors are implicit in satellite derived winds, and the magnitude of these errors is difficult to assess because of the lack of ground truth or verification data. In application of sequential satellite imagery for wind determination, it is assumed that the clouds or water vapor features are conservative passive tracers of the wind field and the motion is also assumed to be only advective. However, this is not always the case and changes in clouds and water vapor features may be misinterpreted and lead to wind errors. Other sources of errors generally fall into two categories: image navigation and registration errors, and feature identification and tracking errors. Because the nature of these sources is understood however, quality and control procedures can be used to reduce errors. Errors attributed to improper height assignment are not actually errors in the wind vectors but in their assignment to a pressure-height coordinate system and subsequent comparison with point source ground truth data (radiosondes or model analyses) and are not discussed in this paper.

2.3 Estimation of wind errors

Also unique to this study is the use of statistical structure functions to independently quantify the random error associated with the wind data set without reference to rawinsonde or modeled wind data. Hillger and Vonder Haar (1988) and Fuelberg and Meyer (1986) and others have shown that structure function analysis can be used to estimate the magnitude of mean non-direction gradients (structure) in data fields. The slope of the structure curves at small separation intervals can be used in the error estimation. The reduction in this random error associated with the use of various quality and control parameters is used as a measure of success for the quality and control parameters.

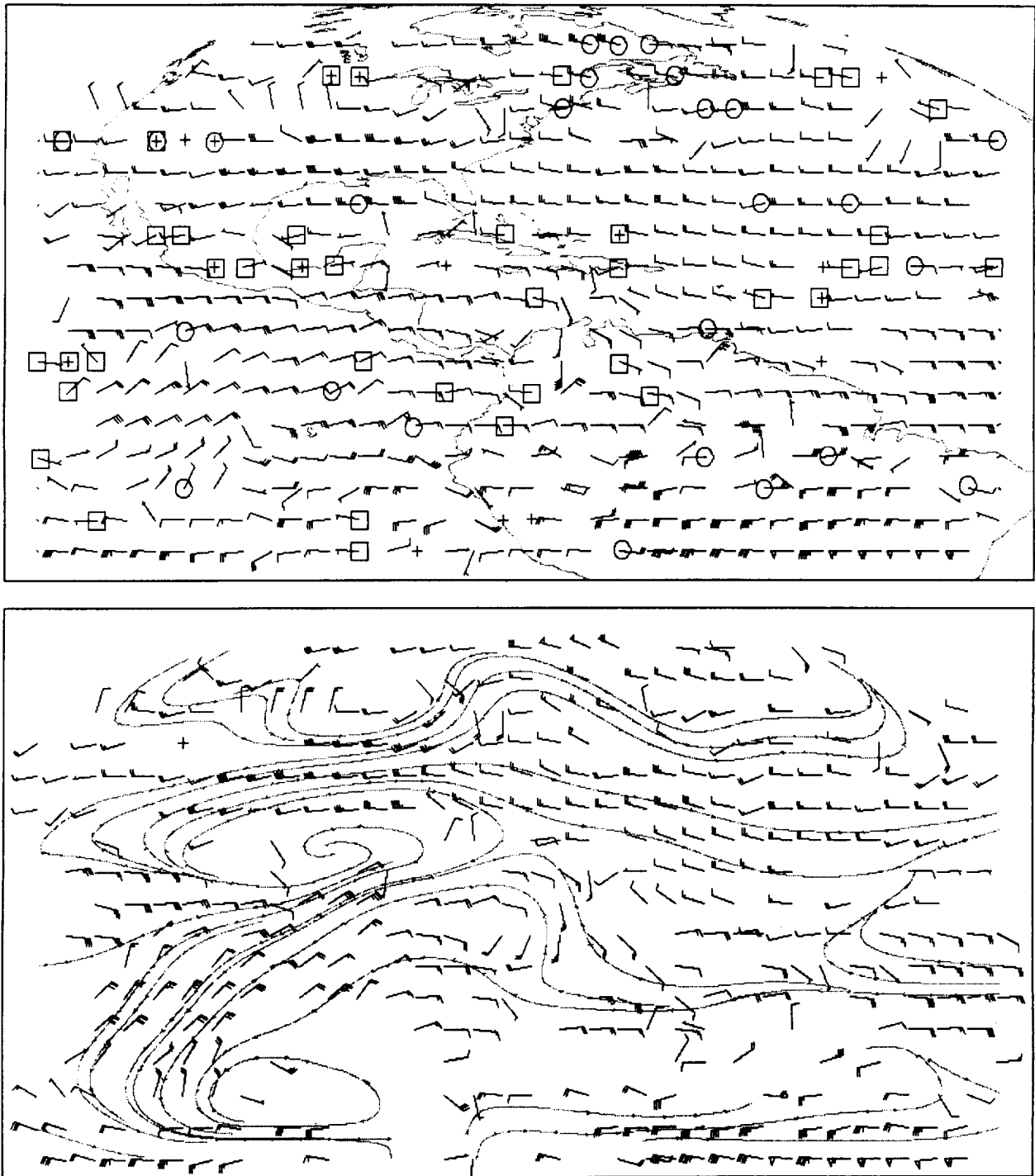


Figure 1. GOES 8 imager water vapor derived winds for June 27, 1995. A sequence of three hourly water vapor images centered around 1515 UTC was used for wind determination. The upper figure (a) presents all wind vectors derived from the tracking algorithm. The vectors in circles and boxes are winds which may or may not be “bad” based on different quality and control methods. The lower figure (b) presents “good” winds as determined by direction and speed deviations of 25° and 10ms^{-1} , respectively. A streamline analysis presents a smooth flow field.

2.4 The height assignment problem

The "height" assignment of water vapor winds is important for a quantitative analysis of the wind field. The GOES 8 imager 6.7 μm channel weighting function peaks between 200 and 600 mb, and its width of significant contribution varies between 200 and 400 mb for cloud-free situations. Therefore the level assigned to winds derived from the water vapor imagery can vary over this range. The height assignment approach used in this study is consistent with other water vapor wind studies and uses the water vapor image brightness temperature and a representative thermodynamic reference profile to assign a pressure height to the wind vectors. The need for more sophisticated CO_2 "slicing" methods (Menzel et al. 1983) may be necessary if clouds are tracked in the water vapor imagery.

3. WIND RESULTS

3.1 Selection of quality and control parameters

Current efforts are focused on examining a number of quasi-objective parameters to evaluate their usefulness in determining good winds from bad ones. The list includes template parameters implicit to the MAW technique (e.g., difference minimums, primary versus secondary minimums, and minimums near the edge of the search area), other easily obtained template parameters (e.g., variance over the template), and template consistency checks between pairs of collocated wind vectors (when 3 sequential images are used for tracking). Recent results indicate that while template minimum differences are a measure of the goodness of fit in tracking an image feature (perfect fit yields a zero difference), a unique threshold applicable throughout the image sequence is not easily discernible. Image variance is useful in identifying regions with limited structure and a threshold can be determined which is applicable for a variety of image sequences. However, the most useful parameters are those derived from consistency checks of two wind vectors derived from a sequence of 3 images. This approach is not unique and has been used to determine a U and V wind component threshold which ranges between 5 and 20 ms^{-1} (Merrill et al. 1991; Laurent 1993; Schmidt and Hayden 1992; and others). Deviations of the U and V components of the wind are not necessarily the best parameters however because they do not significantly account for large directional mismatches at low wind speeds or relatively small directional changes for large displacements (wind speeds). Both of these types of tracking errors regularly occur in water vapor imagery

and are not flagged as bad by the U and V wind component threshold tests.

To test this hypothesis, water vapor winds were calculated for three days using a sequence of three consecutive images. Instead of using u and v components of the wind, differences in the wind speed and direction between two pairs of vectors (calculated from three images) were calculated for each wind vector location. Using subjective evaluation, thresholds were established for the speed deviations which eliminated the bad wind vectors. Bad vectors were determined by looking for spatial continuity between winds and by looping the sequence of imagery for the given case study day. Based on this preliminary work, a speed deviation (ΔS) value of 10 ms^{-1} was determined to be best at eliminating bad wind vectors. Directional deviations (ΔD) between 25° and 45° were also determined effective. Additionally, image variance over the template was evaluated as well and was useful for identifying areas with limited structure. These areas often provided bad wind vectors as well. Variance thresholds can also be used to separate pure water vapor winds from clouds tracked in the water vapor imagery.

3.2 Structure function results

As a benchmark for measuring improvement in water vapor wind vectors, a structure function analysis of the wind components in Figure 1a was made along with those of two other case studies. A U wind component structure function plot for June 27, 1995 is shown in Figure 2 (upper curve). The figure indicates that structure (gradient) increases with increasing separation distance. The steepest slopes corresponded to the scales at which significant gradients in the zonal wind component occur. The intercept of the regression line through the structure curves corresponds to twice the error variance of the data. Therefore the random error in the U component of the wind is calculated as the square root of half the intercept. Random errors for the three days range from 4.18 - 5.66 ms^{-1} when all winds are considered (Table 1). When the direction and speed deviation thresholds are employed a significant number of "bad" vectors are removed and the resulting structure analysis yields the lower curve in Figure 2. Structure at small separation intervals is significantly reduced and the noise inherent in the data is likewise dampened. The random noise values estimated from structure analysis for the improved wind data set are shown in the last column of Table 1. Values range between 0.00 and 3.26 ms^{-1} .

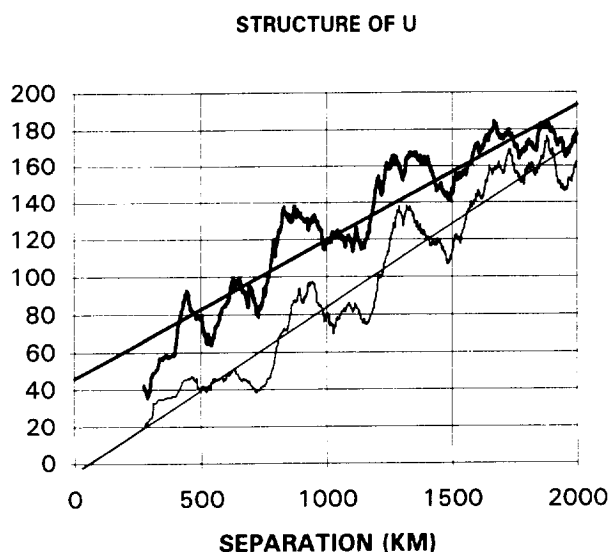


Figure 2. Structure function curves for the U component of the wind on June 27, 1995. The upper curve represents unfiltered winds and the lower curve represents values after quality and control parameters were used to eliminate bad wind vectors. Linear regression lines are also presented. Structure values are in $(\text{ms}^{-1})^2$.

Table 1. Random wind errors determined from structure function analysis. Values in ms^{-1} .

DATE		ALL WINDS	QC WINDS		
			$\Delta U < 5$ $\Delta V < 5$	$\Delta D < 45$ $\Delta S < 10$	$\Delta D < 25$ $\Delta S < 10$
95094 4/4/95	# Vec.	423	298	349	277
	U	5.33	2.38	3.58	1.83
	V	4.18	3.13	3.30	3.13
95178 6/27/95	# Vec.	539	402	426	352
	U	4.73	1.59	3.03	0.00
	V	4.13	2.75	2.93	2.53
95234 8/22/95	# Vec.	535	429	447	361
	U	5.66	3.12	4.02	3.26
	V	4.18	3.06	3.30	2.80

Table 1 also shows the error values when other quality and control parameters are imposed. The middle column corresponds to the wind errors when vector pair constraints of 5 ms^{-1} on either the U or V component are imposed (this is what is typically used operationally). A significant reduction in the random error occurs over the original wind vectors. In most cases this reduction is not as large as for the $\Delta D/$

ΔS thresholds. Discrepancies between these approaches are highlighted in Figure 1. The circled vectors indicate winds which past the 5 ms^{-1} U/V threshold but not the $\Delta S/\Delta D$ one. Vectors in the squares indicate the opposite. This will be the subject of future work and discussed at the conference. The lower plot in Figure 1 (b) indicates the good wind vectors and corresponding streamline analysis for winds passing the $\Delta S/\Delta D$ threshold limits.

References

- Atkinson, R. J., 1987: Automated mesoscale winds determined from satellite imagery. *Final Report on NAS8-34596*, General Electric Company, Huntsville, AL, 50 pp.
- Barnea, D. I., and H. F. Silverman, 1972: A class of algorithms for fast digital image registration. *IEEE Transactions on Computers*, C-21, 179-186.
- Fuelberg, H. E., and P. J. Meyer, 1986: An analysis of mesoscale VAS retrievals using statistical structure functions. *J. Clim. Appl. Meteor.*, 25, 59-76.
- Hayden, C. M., and C. S. Velden, 1991: Quality control and assimilation experiments with satellite-derived wind estimates. *Preprints Ninth Conference on Numerical Weather Prediction*. Amer. Meteor. Soc.
- Hayden, C. M., and T. J. Schmidt, 1992: Quantitative applications of the $6 \mu\text{m}$ water vapor band measurements from satellites. *Preprints Sixth Conference on Satellite Meteorology and Oceanography*, Amer. Meteor. Soc., Atlanta, 188-192.
- Hillger, D. W. and T. H. Vonder Haar, 1988: Estimating noise levels of remotely sensed measurements from satellites using spatial structure analysis. *J. Atmos. Ocean. Technol.*, 5, 206-214.
- Laurent, H., 1993: Wind extraction from Meteosat water vapor channel image data. *J. Appl. Meteor.*, 32, 1124-1133.
- Menzel, W. P., W. L. Smith, and T. R. Stewart, 1983: Improved cloud motion wind vector and altitude assignment using VAS. *J. Clim. Appl. Meteor.*, 22, 377-384.
- Merrill, R. T., W. P. Menzel, W. Baker, J. Lynch, and E. Legg, 1991: A report on the recent demonstration of NOAA's upgraded capability to derive cloud motion satellite winds. *Bull. Amer. Meteor. Soc.*, 72, 372-376.
- Wilson, G. S., 1984: Automated mesoscale wind fields derived from GOES satellite imagery. *Preprints Conference on Satellite Meteorology/ Remote Sensing and Applications*. Amer. Meteor. Soc., Clearwater, 164-171.

